Nanotechnology **23** (2012) 015201 (8pp) doi:10.1088/0957-4484/23/1/015201

Charged excitons, Auger recombination and optical gain in CdSe/CdS nanocrystals

Marco Marceddu[1], Michele Saba[2], Francesco Quochi[2], Adriano Lai[3], Jing Huang[4], Dmitri V Talapin[4], Andrea Mura[2,5] and Giovanni Bongiovanni[2,5]

[1] Centro Grandi Strumenti d'Ateneo, Università di Cagliari, I-09042 Monserrato (CA), Italy
[2] Dipartimento di Fisica, Università di Cagliari, I-09042 Monserrato (CA), Italy
[3] Istituto Nazionale di Fisica Nucleare, Sezione di Cagliari, I-09042 Monserrato (CA), Italy
[4] Department of Chemistry, University of Chicago, Chicago, IL 60637, USA
[5] Istituto Officina dei Materiali del Consiglio Nazionale delle Ricerche (CNR-IOM) Unità SLACS, I-09042 Monserrato (CA), Italy

E-mail: michele.saba@dsf.unica.it

Received 4 September 2011, in final form 31 October 2011
Published 8 December 2011
Online at stacks.iop.org/Nano/23/015201

Abstract
CdSe/CdS colloidal nanocrystals are members of a novel class of light-emitting nanoparticles with remarkable optical properties such as suppressed fluorescence blinking and enhanced emission from multiexciton states. These properties have been linked to the suppression of non-radiative Auger recombination. In this work we employ ultrafast spectroscopy techniques to identify optical signatures of neutral and charged excitonic and multiexcitonic states. We show that Auger recombination of biexcitons is not suppressed, while we observe optical gain and amplified spontaneous emission from multiexciton states and from long-lived charged-exciton states.

S Online supplementary data available from stacks.iop.org/Nano/23/015201/mmedia

(Some figures may appear in colour only in the online journal)

1. Introduction

Colloidal nanocrystals (NCs) are promising nanomaterials for solution-processable photonic and optoelectronic devices. The energy level spectrum and thus the optical properties of NCs can be tailored at the synthesis stage, controlling composition, size and engineering the shape. Composite, heterostructured nanocrystals have been grown in a large variety of sizes and shapes, spanning from spherical core/shell nanocrystals, to elongated dot/rod and multi-branched geometries, with both types I and II band alignments that provide an efficient way to engineer the charge carrier wavefunctions and their interactions [1, 2]. Successful applications have been established in the field of fluorescent biological markers and light-emitting diodes and, thanks to such a level of control, several others seem within reach, including single-photon sources, solar cells, photodetectors and lasers [3].

Concerning optoelectronic applications, non-radiative recombination phenomena have represented a significant roadblock towards successful exploitation of NC properties. Whenever multiexciton or charged excitons are generated in NCs, Auger recombination occurs, a process in which, due to the Coulomb interaction, one exciton disappears by conferring its entire energy to another exciton in the NC [4]. As a result of Auger recombination, the excited-state lifetime, typically of the order of 10 ns for single-exciton states, can be reduced to hundreds of ps or less for multiexcitons or charged excitons, a detrimental effect if excitons are to be exploited for optical emission or photoconversion [5]. Fast Auger recombination has been linked to a variety of unwanted optical phenomena in NCs: blinking of photoluminescence, ultrashort optical gain lifetime and narrow bandwidth for optical gain. Blinking of photoluminescence occurs when NCs are continuously illuminated, meaning that nanocrystals can be bright or dark for alternating periods of times [6]. The very origin of blinking is still debated. It was originally proposed that dark periods correspond to NCs with an extra charge in the core. Such NCs appear 'dark' under illumination as light absorption would result in a charged state unable to emit light owing to fast Auger decay.

The recent demonstration of core/shell NCs engineered to be blink-free has therefore represented an important advance [7–10]. Such nanocrystals were grown with the core overcoated by a thick shell (and therefore called giant core/shell NCs), with a resulting graded heterostructure, meaning that the two semiconductors constituting the inner core and the outer shell formed an alloy at the interface. The confining potential for electrons and holes was smoother than in the case of an abrupt interface, a feature that theoretical calculations and measurements have indicated as crucial in reducing Auger recombination and blinking [11, 12]. The reduced blinking was accompanied in a variety of similarly designed nanocrystals by efficient multiexciton photoluminescence emission, even under cw excitation, and multiexciton decay times that have been interpreted as evidence for suppression of Auger recombination [10, 13–16]. Earlier reports on similar nanocrystals, however, seemed to imply that the lifetime of biexcitons in CdSe/CdS nanocrystals is much shorter than 1 ns [17–20], a finding directly in contrast with the notion of suppressed Auger recombination. The role played by surface defects should also be considered, since it has been proved that surface traps significantly affect exciton and multiexciton recombination dynamics [21–26]. Indeed it was recognized that selective excitation of specific excitonic states provides efficient and large gain development, also in NCs that were believed to show zero gain [22–25], while surface-induced processes may lead to misinterpretation of the NC dynamics [26]. Moreover recent experiments have measured the decay time and efficiency of the optical emission from charged states [27–33], showing efficient emission from charged-exciton states even in blinking nanocrystals and therefore questioning the very link between charged states and blinking. Understanding the optical properties of charged states is crucial not only to prevent blinking, but also to design optoelectronic NC-based devices that need to work in the presence of free charges, such as electrically pumped LEDs and lasers, or efficient photodetectors and solar cells. Therefore, due to the complexity of Auger multiparticle interaction, surface-induced processes and charged-states dynamics, it is very important to generalize the arguments by studying different material designs with complementary experimental and theoretical techniques.

In the present work we set up ultrafast spectroscopy experiments to spectrally and temporally separate exciton, charged excitons, biexciton and multiexciton optical transitions in CdSe/CdS core/shell NCs and directly measure in the time domain their lifetimes. Our time-resolved photoluminescence and transient absorption measurements directly accessed the lifetime of such excited states, providing a clear picture of Auger phenomena in CdSe/CdS NCs and highlighting the role played by surface defects, also in giant core/shell NCs.

2. Experimental details

Time-resolved photoluminescence (TR-PL) measurements were performed by means of a streak camera (Hamamatsu C5680-N5716), coupled to a grating spectrograph (Acton SpectraPro 2300i). A kilohertz-repetition rate regenerative amplifier (Quantronix Integra C) provided the pulsed laser excitation, 150 fs in duration; a parametric amplifier (LightConversion Topas) converted the laser wavelength to 500 nm. Laser light was focused on a 300 μm spot, ensuring uniform excitation of the NC solution contained in a 1 mm quartz cuvette; photoluminescence was collected from the central part of the excited spot with a 100 mm focal lens. Temporal resolution was 90 ps for spectrograms with a 20 ns time range and 25 ps in scans with 2 ns range.

Femtosecond transient absorption measurements were performed by employing a two-color pump–probe technique, using the same laser as for PL measurements. Pump excitation wavelengths at 392 and 500 nm were used, while the white-light supercontinuum probe beam was generated by focusing laser pulses on a sapphire plate. Pump and probe beams crossed with a 2° angle on the NC cuvette with a 1 mm waist. The pump beam was chopped at 500 Hz, synchronously with the laser repetition rate, while the spectrum of individual probe pulses was detected at a 1 kHz rate with a 16-bit CCD camera (Andor Newton) coupled to a grating spectrometer (Acton SpectraPro 2300i).

3. Results and discussion

Giant CdSe/CdS NCs were prepared by seeded growth [7, 33–36]. 3.6 nm CdSe cores were covered with a thick CdS shell up to a total size of 8–10 nm (see the TEM image in figure 1). Absorbance and photoluminescence (PL) spectra of NCs dispersed in toluene are shown in figure 1. The PL was centered around 630 nm, a wavelength corresponding to emission from the CdSe core, meaning that optical excitations relaxed to the lowest-energy states before emitting. The absorption features reflected instead the core/shell volume ratio, with the peaks at wavelengths longer than 500 nm pertaining to absorption directly into the CdSe core and the absorption at wavelengths shorter than 500 nm occurring mostly in the CdS shell.

The band alignment at the CdSe/CdS interface has long been debated in the literature: while the valence band offset is large enough to assume that holes are certainly confined into the CdSe core, the conduction bands are very close to each other so that the exact alignment depends on the relative sizes of core and shell as well as on interfacial strain and dipole effects [7, 19, 36–38, 18, 39, 40]. In any case the confinement for electrons is very shallow and the alignment is often termed ‘quasi type II’, to indicate that electron wavefunctions in the conduction band significantly leak into the shell volume.

Figure 2 shows the spectrogram from CdSe/CdS NCs excited at 500 nm at the largest accessible pump fluence. The lowest-energy optical transition, 630 nm in wavelength, was similar in nature to the fundamental transition in core CdSe nanocrystals. For our purposes, the lowest-energy excitonic transitions can be described in terms of a two-level system with doubly degenerate electron and hole levels [41]. The emission at lower wavelengths, centered at 580 nm, was instead attributed to multiexciton states of order higher than 2. The left-side panel contains the PL spectra for increasing delay time after pump excitation; spectra A–C were obtained

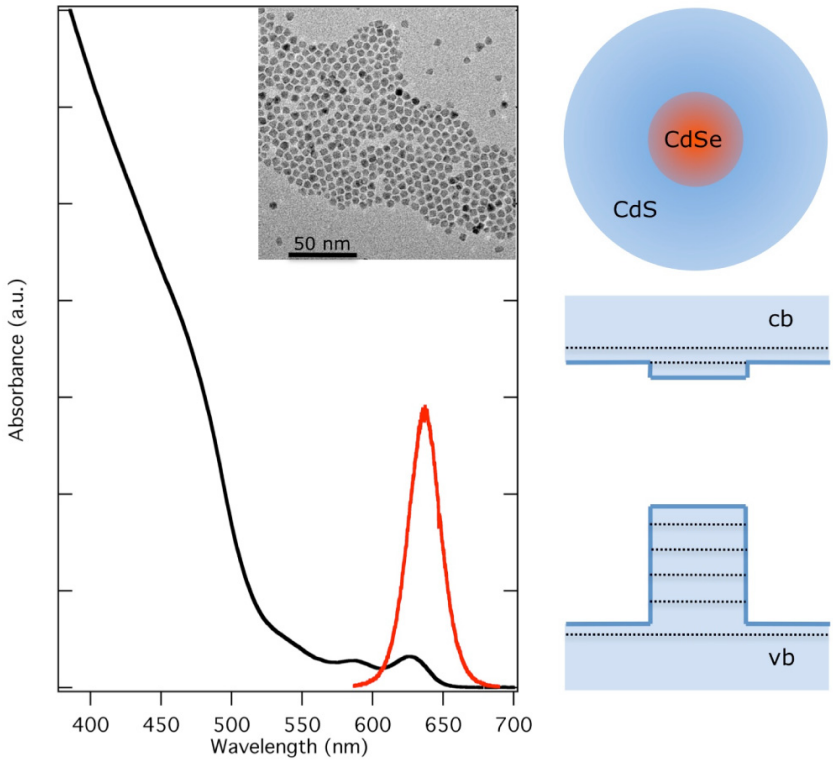

Figure 1. Left: absorbance (black line) and photoluminescence (red line) spectra of CdSe/CdS nanocrystals. Inset: TEM image of nanocrystals. Right: sketch of the nanocrystal composition and energy levels.

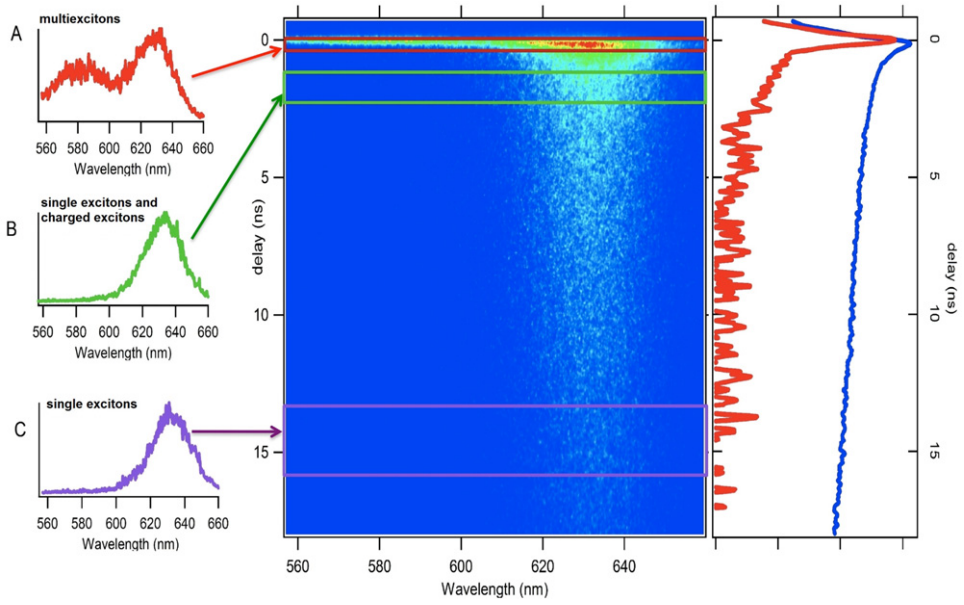

Figure 2. Spectrogram of time-resolved photoluminescence over a 20 ns time range with 90 ps resolution from CdSe/CdS nanocrystals for a laser fluence of 5 mJ cm^{-2}. Left-side panel: photoluminescence spectra as a function of time delay with respect to the laser pulse ((A) delay 0 ns, integrated in a 50 ps gate; (B) delay 1 ns, gate 1 ns; (C) delay 13 ns gate 3 ns). Right-side panel: time decay of the photoluminescence signal measured at 630 nm (blue trace corresponding to exciton and biexciton emission) and at 580 nm (red trace corresponding to multiexciton emission).

integrating the streak images in the time windows labeled accordingly. Immediately after excitation, the average exciton population per NC was above 10 and distributed according to Poisson probabilities; the corresponding PL spectrum contained emission both at 630 and 580 nm. As illustrated in the right-side panel, the multiexciton emission decayed faster than the experimental resolution. High-resolution PL spectrograms confirmed that the multiexciton state lifetime

was shorter than 25 ps. Therefore the PL spectrum measured 100 ps after excitation (B) contained no emission from states with three or more excitons, even at the highest available excitations. In the limit of high excitation, the fast multiexciton Auger recombination transformed within 25 ps the initial Poissonian distribution of excitations into a distribution of biexcitons and excitons. In this regime, however, the PL signal kept decaying with a sub-nanosecond time constant, direct evidence of non-radiative Auger recombination of biexciton states, even in these core/shell NCs. Several nanoseconds after excitation, only singly occupied NCs were emitting and the single-exciton 18 ns decay time was recovered, as clearly illustrated by the temporal trace in the right-side panel of figure 2. The fluorescence lifetimes of multiexcitons, biexcitons and single excitons differ from each other by about one order of magnitude, providing a tool to resolve emissions arising from different excited states.

A closer inspection of the 630 nm PL band shown in figures 2(a)–(c) (see supplementary information available at stacks.iop.org/Nano/23/015201/mmedia) reveals that multiexciton emissions are blueshifted with respect to single-exciton emission, thus indicating repulsive exciton–exciton interaction, with a resulting biexciton binding energy of the order of 10 meV.

Figure 3 reports the spectral shift of the 630 nm PL peak as a function of time. Since the shift was caused by exciton–exciton interactions [19], it could only be present as long as NCs were multiply excited and tracking its dynamics reflected the dynamics of NCs containing two or more excitons. The shift was obtained from TR-PL spectrograms by marking the center of a Gaussian curve fitting the 630 nm band in each spectrum and calculated with respect to the band maximum wavelength observed at the lowest excitation level, when PL is entirely due to single excitons. The shift immediately after the excitation pulse was towards the blue as a consequence of the repulsive exciton–exciton interaction [19]. The initial sub-nanosecond decay of the shift (see the inset for a high-temporal resolution blow-up of the first nanosecond dynamics) hinted at the fast Auger recombination of biexciton states. Other effects, in particular self-absorption, could be expected to cause similar ultrafast PL shifts as the exciton population relaxes, independently of the biexciton interaction sign. However, the same measurements performed on control samples, namely a toluene dispersion of CdSe/ZnS core/shell nanocrystals from Evident Technologies, emitting at 620 nm, showed that the ultrafast PL shift had a positive sign, following the attractive exciton–exciton interaction in such samples (see supplementary information for the data available at stacks.iop.org/Nano/23/015201/mmedia), suggesting that biexciton states are indeed the main reason for the observed transient spectral shifts.

After the initial sub-nanosecond decay, the PL shift did not disappear, but changed its sign and a small redshift was left over for several ns, until the single-exciton emission spectrum was recovered. The experimental data did not allow a definitive attribution of such a residual shift observed between 1 and 8 ns delay: contributions from ultrafast thermalization effects could not be ruled out, but it is also possible that the shift was caused by different exciton species.

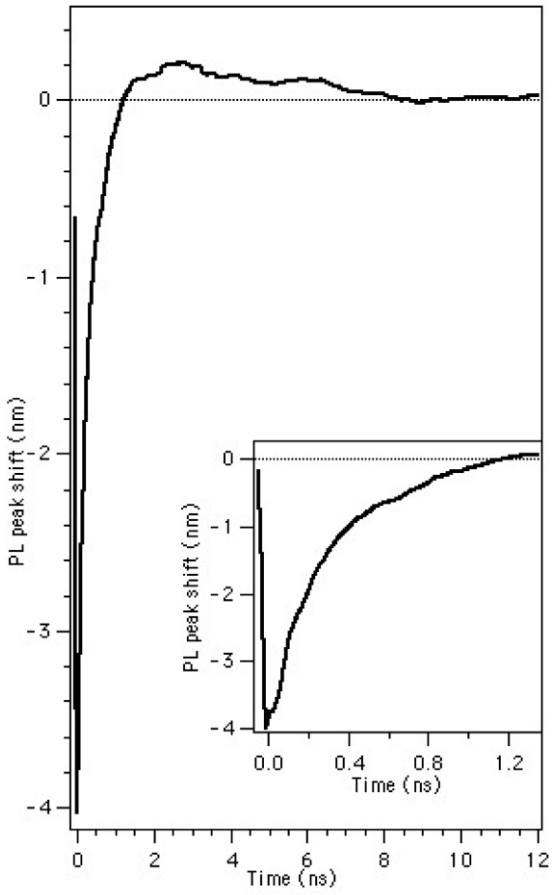

Figure 3. Temporal evolution of the spectral shift of the 630 nm PL peak extracted from the streak-camera spectrogram; the inset shows a magnification of the first nanosecond dynamics (temporal resolution: 25 ps).

In figure 4 the PL time decays for varying pump fluences are compared for our CdSe/CdS NCs and for a solution of commercial CdSe/ZnS core/shell NCs (Evident Technologies Evidot 620) as a reference, well known to present fast Auger recombination of multiexciton and biexciton states. At low pump fluence, the PL monitored at 630 nm in CdSe/CdS NCs showed a single exponential decay with a 18 ns decay constant, characteristic of single-exciton fluorescence. The PL signal of reference NCs decayed with a single-exciton 9 ns lifetime and always showed a slightly faster initial transient. By increasing the excitation level, we observed an initial sub-nanosecond decay both in CdSe/CdS and reference samples; however, CdSe/CdS NCs differed from the reference NCs due to the presence of a third component in the PL decays, which could be clearly identified in the range between 2 and 5 ns, which was much weaker in reference NCs.

We extracted the three components of the CdSe/CdS NC PL decays by fitting the curves with the sum of three exponential decays with characteristic times, respectively 150 ps, 1.6 ns and 18 ns (see the supporting material paragraph for details on the fitting procedure available at stacks.iop.org/Nano/23/015201/mmedia).

Figure 5 shows how the amplitudes of the three components evolved with the excitation level. Measurements

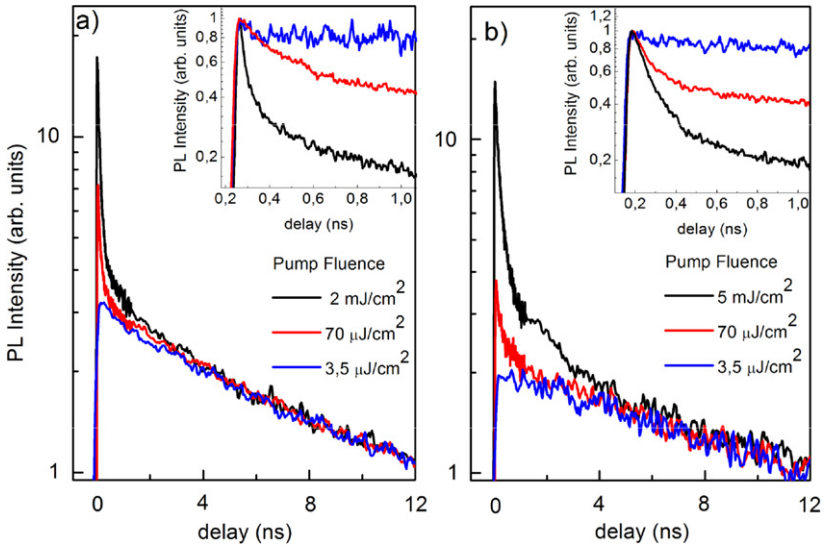

Figure 4. Time-resolved PL from CdSe/ZnS Evidot 620 NCs (panel (a)) and CdSe/CdS NCs (panel (b)) measured in a ∼10 nm spectral band around the exciton peak; the decays were scaled so that they overlapped at long delays; in the insets are shown blow-ups of the decay in the first nanosecond after excitation and decays were normalized to 1.

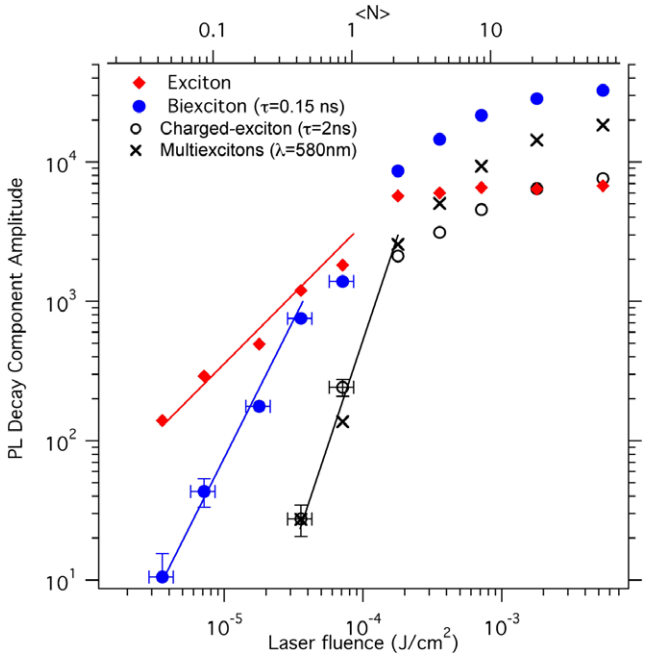

Figure 5. Dependence on laser power of the three components of photoluminescence decays and of multiexciton emission. The three components were extracted from the fitting procedure on decays of the emission at 630 nm in wavelength, as described in the text. The multiexciton emission was instead extracted from the amplitude at time 0 of the emission at 580 nm in wavelength. The red, blue and black lines represent a linear, quadratic and cubic behavior, respectively. Vertical error bars represent statistical errors on multiexponential fitting parameters, horizontal error bars are to be attributed to laser intensity fluctuations and to inhomogeneities on the power meter surface (for clarity, horizontal error bars are displayed only for a few points, but the uncertainties are proportional to the laser fluence and therefore significant for all points in the plot).

were taken in random order of laser power and successive measurements were separated by a ≈100 s delay during which the sample was kept in the dark, in order to avoid, as far as possible, charging effects due to prolonged nanocrystal irradiation. Different series of measurements taken in different orders yielded almost indistinguishable results. The 18 ns component, attributed to single-exciton decay, grew linearly before saturating. The faster 150 ps component appeared second and initially had quadratic growth with the laser power; for such a reason it is natural to attribute this component to biexciton recombination. The third component, with the intermediate 1.6 ns decay time, appeared last and initially grew super-linearly, approximately as the third power of the excitation intensity, with the same dependence as multiexciton states with at least three excitons. As multiexciton states had a much shorter lifetime (less than 0.1 ns versus 1.6 ns), it seemed reasonable to attribute such a component to charged-exciton states created as a by-product of Auger recombination of multiexciton states and charge-trapping events [28, 32]. Our interpretation was corroborated by the fact that such a component appeared only at higher pumping; as a further link between multiexciton and charged-exciton states, the optical emission at 580 nm, attributed to multiexcitons, had an initial growth as a function of laser energy very similar to the growth of the charged-exciton component (see figure 5). We could not exclude contributions to charged-exciton formation from long-lived charged states surviving from one pulse to the next, although the observed trends as a function of the excitation power were evidence that most of such states were created with a single laser pulse. Various kinds of charged excitons were reported in the literature, depending on whether the missing charge ends trapped at a surface defect or freely leaves the NC [22, 26]. The collected data did not allow us to speculate on the nature of the observed charged-exciton state; however, since a single exponential decay component was attributed to charged exciton, we may exclude contributions from an inhomogeneous collection of different traps.

In order to measure the gain properties of our nanocrystals and correlate them with the observed multiexciton dynamics, we set up femtosecond transient absorption measurements able

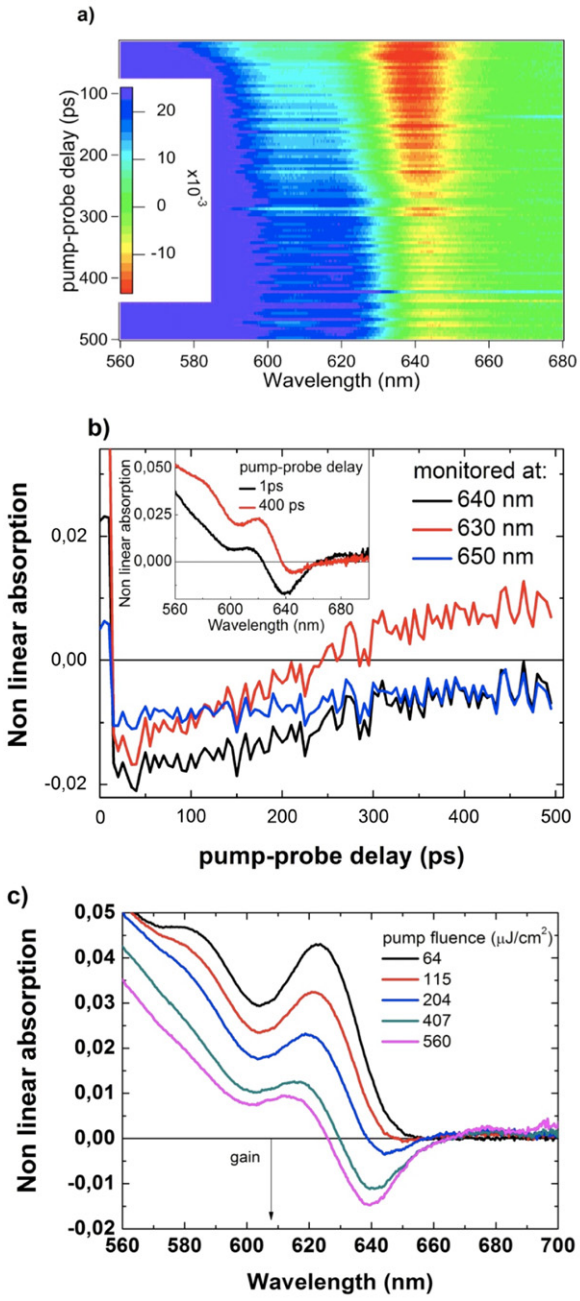

Figure 6. (a) Nonlinear absorption spectrogram; (b) gain lifetime measured at different wavelengths at the largest excitation level; in the inset is the full spectrum immediately after pump excitation (delay 0) and for 400 ps delay time; and (c) nonlinear absorption spectra as a function of the pump fluence.

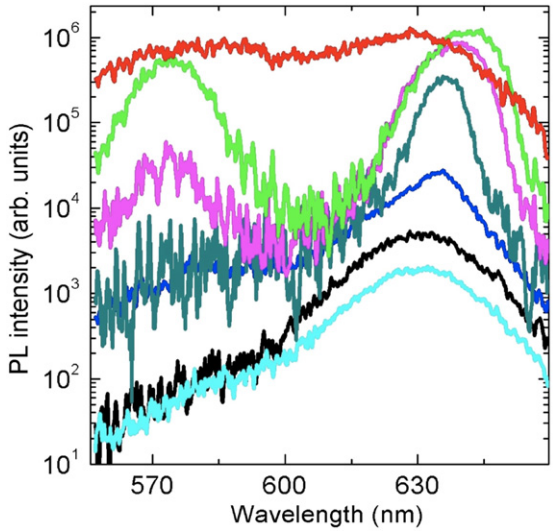

Figure 7. TR-PL spectra as a function of laser fluence showing ASE development; spectra were time-integrated in a 50 ps wide domain; pump fluences were 17 μJ cm^{-2} (turquoise), 35 μJ cm^{-2} (black), 180 μJ cm^{-2} (blue), 360 μJ cm^{-2} (dark green), 3.5 mJ cm^{-2} (violet) and 5.3 mJ cm^{-2} (green); the solution PL spectrum at the maximum pump level (red trace) is also shown for bandwidth comparison.

to directly track the bleaching of optical transitions due to excitons or individual carriers in NCs (see supporting material for nonlinear absorption calculation details available at stacks.iop.org/Nano/23/015201/mmedia). Bleaching was observed in the low-excitation regime for all optical transitions in the absorption spectrum, even the ones pertaining to the CdS shell, a feature associated with delocalization of electrons in the NC [18] (see the supporting material paragraph for differential transmission spectra where transitions could be identified available at stacks.iop.org/Nano/23/015201/mmedia).

In figure 6 are the plots of the nonlinear absorption spectra for various pump fluences: for pump fluences exceeding 115 μJ cm^{-2}, negative absorption, corresponding to optical gain, was observed at about 640 nm. By further increasing the pump fluence, the gain bandwidth increased and a blueshift was observed. Remarkably, even at the largest pump fluence, optical gain did not occur at the biexciton emission wavelength, but was systematically redshifted, suggesting that charged-exciton and single-exciton states may contribute to optical gain. This hypothesis was confirmed by the gain dynamics, as the initial fast decay was followed by a much longer one, so that 400 ps after the excitation gain could still be sustained. Moreover the dynamics depended on wavelength: the fast component was more important on the blue side of the exciton resonance, where the biexciton component was expected to be more important, while on the red side of the resonance, where single- and charged-exciton transitions dominated, the decay was slower.

TR-PL measurements (figure 7) on NC films prepared by a solution drop-cast on a glass slide showed significant changes in the fluorescence spectrum as a function of excitation fluence. For a threshold laser fluence around 100 μJ cm^{-2} a new sharp emission was observed at about 640 nm, superimposed on the 630 nm PL band. In contrast to the 630 nm wide band, whose intensity saturated for large fluences, the intensity of this new sharp emission showed super-linear dependence on pump fluence. Monitoring the PL decay at 640 nm revealed a very fast build-up and decay, with time constants below the temporal resolution achievable with the PL measurement set-up. Thus the 640 nm emission was a clear signature of amplified spontaneous emission (ASE). Upon further increase of the excitation level, ASE was observed also at 575 nm, thus indicating stimulated emission from multiexciton states, similar to what was observed in [13]; under

the same conditions, the emission around 640 nm shifted to the red and broadened. The redshifted ASE, with respect to exciton and multiexciton fluorescence, has to be related to the gain band profile. Indeed ASE developed in the spectral region of largest overlap between fluorescence and gain (see supplementary information for a closer comparison available at stacks.iop.org/Nano/23/015201/mmedia). Experimental and theoretical studies showed that charged excitons are redshifted with respect to both biexcitons and single excitons [32, 42]. It should be observed, however, that, depending on excitation wavelength, different excitonic states may be accessed, with different multiexciton interactions, resulting in similar redshifted ASE and gain [23].

Very recent reports on biexciton quantum yield on NCs implied, in agreement with our interpretation, that biexciton and charged-exciton Auger recombination lifetimes were very different [43], i.e. that biexciton states recombined much faster than charged-exciton ones. Such charged excitons were likely created by Auger recombination and charge trapping in our experiments, and would therefore appear in any optically pumped NC laser.

Since our measurements did not allow the univocal identification of the nature and formation mechanism of the charged states, dedicated and systematic optical spectroscopy measurements are currently underway to identify charge-trapping mechanisms, determine trap lifetimes and depths as well as trapping yields.

It is worthwhile to compare our results with previously reported findings about similar core/shell systems. ASE from multiexcitons, the nonlinear ns component in the PL decay and the long tail of the transient absorption decay in CdSe/CdS heterostructured NCs has been recently attributed to the suppression of multiexciton and biexciton Auger recombination [12–15]. In our samples, such experimental observations coexisted with fast Auger recombination of biexciton and multiexciton states, while the longer decay of PL emission and optical gain should be attributed to charged-exciton states. Although our synthesis procedures were similar to the ones reported in the literature, the CdSe/CdS interface in our NCs could be more abrupt, so that it did not inhibit Auger recombination of biexcitons. On the other hand, single NC studies even highlighted that the same synthesis could lead to different optical nonlinearities. This doubt highlights once more the importance of gathering a reliable control of the potential barrier at the core/shell interface [11, 12] and, given the vast implications of Auger processes, warrants further experiments on samples with different sizes and morphologies.

4. Conclusions

In this work we have studied the optical properties of CdSe/CdS core/shell NCs by means of time-resolved ultrafast spectroscopy. By the comprehensive analysis of the spectral features and temporal dynamics we identified signatures of four different exciton states: multiexcitons, biexcitons, single excitons and charged excitons. The sub-nanosecond decay lifetime of multiexcitons and biexcitons revealed fast Auger recombination, that instead is less efficient in the decay pathway of charged excitons. Different exciton states were found to contribute to optical gain and amplified spontaneous emissions, with charged excitons as the leading source of the 400 ps long gain. The slow Auger recombination of charged excitons and the long-lived gain are findings of very important consequence for the prospects of a cw NC laser.

Acknowledgments

This work was partially funded by MIUR through FIRB projects (Synergy-FIRBRBNE03S7XZ and FIRB-RBAU01N449), by the European Commission through the Human Potential Programs (RTN Nanomatch, contract no. MRTN-CT-2006-035884) and by the Regione Autonoma della Sardegna trough PO-FSE Sardegna 2007–2013, LR 7/2007 'Promozione della ricerca scientifica e dell'innovazione tecnologica in Sardegna', 'Borse Giovani Ricercatori' (supporting MM) and through the project 'Design di nanomateriali ibridi organici/inorganici per l'energia fotovoltaica', 'Progetti di Ricerca Fondamentale'.

References

[1] Yin Y and Alivisatos A P 2005 *Nature* **437** 664
[2] Rogach A L (ed) 2008 *Semiconductor Nanocrystal Quantum Dots* (NewYork: Springer)
[3] Talapin D V, Lee J-S, Kovalenko M V and Shevchenko E V 2010 *Chem. Rev.* **110** 389
[4] Klimov V I (ed) 2003 *Semiconductor and Metal Nanocrystals: Synthesis and Electronic and Optical Properties* (New York: CRC Press)
[5] Klimov V I, Mikhailovsky A A, McBranch D W, Leatherdale C A and Bawendi M G 2000 *Science* **287** 1011
[6] Nirmal N, Dabbousi B O, Bawendi M G, Macklin J J, Trautman J K, Harris T D and Brus L E 1996 *Nature* **383** 802
[7] Mahler B, Spinicelli P, Buil S, Quelin X, Hermier J-P and Dubertret B 2008 *Nature Mater.* **7** 659
[8] Yongfen Chen Y, Vela J, Htoon H, Casson J L, Werder D J, Bussian D A, Klimov V I and Hollingsworth J A 2008 *J. Am. Chem. Soc.* **130** 5026
[9] Wang X, Ren X, Kahen K, Hahn M A, Rajeswaran M, Maccagnano-Zacher S, Silcox J, Cragg J E, Efros A L and Krauss T D 2009 *Nature* **459** 686
[10] Osovsky R, Cheskis D, Kloper V, Sashchiuk A, Kroner M and Lifshitz E 2009 *Phys. Rev. Lett.* **102** 197401
[11] Cragg G E and Efros A L 2010 *Nano Lett.* **10** 313
[12] Garcia-Santamaria F, Brovelli S, Viswanantha R, Hollingsworth J A, Htoon H, Crooker S A and Klimov V I 2011 *Nano Lett.* **11** 687–93
[13] Garcia-Santamaria F, Chen Y F, Vela J, Schaller R D, Hollingsworth J A and Klimov V I 2009 *Nano Lett.* **9** 3482
[14] Htoon H, Malko A V, Bussian D, Vela J, Chen Y, Hollingsworth J A and Klimov V I 2010 *Nano Lett.* **10** 2401
[15] Zavelani-Rossi M, Lupo M G, Tassone F, Manna L and Lanzani G 2010 *Nano Lett.* **10** 3142
[16] Lutich A A, Mauser Ch, Da Como E, Huang J, Vaneski A, Talapin D V, Rogach A L and Feldmann J 2010 *Nano Lett.* **10** 4646–50
[17] Cretí A, Anni M, Zavelani Rossi M, Lanzani G, Leo G, Della Sala F, Manna L and Lomascolo M 2005 *Phys. Rev.* B **72** 125346
[18] Lupo M G, Della Sala F, Carbone L, Zavelani-Rossi M, Fiore A, Luer L, Polli D, Cingolani R, Manna L and Lanzani G 2008 *Nano Lett.* **8** 4582

[19] Saba M, Minniberger S, Quochi F, Roither J, Marceddu M, Kovalenko M V, Talapin D V, Heiss W, Mura A and Bongiovanni G 2009 *Adv. Mater.* **21** 4942
[20] Mauser Ch, Da Como E, Baldauf J, Huang J, Vaneski A, Talapin D V, Rogach A L and Feldmann J 2010 *Phys. Rev.* B **82** 081306
[21] Kambhampati P 2011 *Acc. Chem. Res.* **44** 1–13
[22] Sewall S L, Cooney R R, Anderson K E H, Dias E A, Sagar D M and Kambhampati P 2008 *J. Chem. Phys.* **129** 084701
[23] Cooney R R, Sewall S L, Sagar D M and Kambhampati P 2009 *J. Chem. Phys.* **131** 164706
[24] Sewall S L, Cooney R R, Anderson K E H, Dias E A and Kambhampati P 2006 *Phys. Rev.* B **74** 235328
[25] Tyagi P, Cooney R R, Sewall S L, Sagar D M, Saari J I and Kambhampati P 2010 *Nano Lett.* **10** 3062–7
[26] Tyagi P and Kambhampati P 2011 *J. Chem. Phys.* **134** 094706
[27] Wang C, Wehrenberg B L, Woo C Y and Guyot-Sionnest P 2004 *J. Phys. Chem.* B **108** 9027
[28] Jha P P and Guyot-Sionnest P 2009 *ACS Nano* **3** 1011
[29] Spinicelli P, Buil S, Quélin X, Mahler B, Dubertret B and Hermier J-P 2009 *Phys. Rev. Lett.* **102** 136801
[30] Gómez D E, van Embden J, Mulvaney P, Fernée M J and Rubinsztein-Dunlop H 2009 *ACS Nano* **3** 2281
[31] Zhao J, Nair G, Fisher B R and Bawendi M G 2010 *Phys. Rev. Lett.* **104** 157403
[32] Louyer Y, Biadala L, Tamarat Ph and Lounis B 2010 *Appl. Phys. Lett.* **96** 203111
[33] Talapin D V, Koeppe R, Goetzinger S, Kornowski A, Lupton J M, Rogach A L, Benson O and Feldmann J 2003 *Nano Lett.* **3** 1677
[34] Talapin D V, Nelson J H, Shevchenko E V, Aloni S, Sadtler B and Alivisatos A P 2007 *Nano Lett.* **7** 2951
[35] Carbone L *et al* 2007 *Nano Lett.* **7** 2942
[36] Dabbousi B O, Rodriguez-Viejo J, Mikulec F V, Heine J R, Mattoussi H, Ober R, Jensen K F and Bawendi M G 1997 *J. Phys. Chem.* B **101** 9463
Peng X, Schlamp M C, Kadavanich A and Alivisatos A P 1997 *J. Am. Chem. Soc.* **119** 7019
[37] Muller J, Lupton J M, Lagoudakis P G, Schindler F, Koeppe R, Rogach A L, Feldmann J, Talapin D V and Weller H 2005 *Nano Lett.* **5** 2044
[38] Steiner D, Dorfs D, Banin U, Della Sala F, Manna L and Millo O 2008 *Nano Lett.* **8** 2954
[39] Sitt A, della Sala F, Menagen G and Banin U 2009 *Nano Lett.* **9** 3470
[40] Lou Y and Wang L-W 2010 *ACS Nano* **4** 91
[41] Norris D J and Bawendi M G 2006 *Phys. Rev.* B **53** 16338
[42] Califano M 2011 *ACS Nano* **5** 3614–21
[43] Nair G, Zhao J and Bawendi M G 2011 *Nano Lett.* **11** 1136